

# Single-pulse ultraviolet laser-induced surface modification and ablation of polyimide

K. Piglmayer, E. Arenholz, C. Ortwein, N. Arnold, and D. Bäuerle<sup>a)</sup>  
*Angewandte Physik, Johannes-Kepler-Universität Linz, A-4040 Linz, Austria*

(Received 16 February 1998; accepted for publication 5 June 1998)

Single-pulse laser ablation of polyimide was investigated by using focused UV-Ar<sup>+</sup>-laser radiation ( $\lambda \approx 302$  nm,  $140$  ns  $\leq \tau_p \leq 50$  ms) and atomic force microscopy. The results clearly demonstrate that the ablation rates do *not* depend on the total dose only, but depend as well on the duration of the laser pulses,  $\tau_p$ . The experimental results can be interpreted almost quantitatively on the basis of a purely thermal model. © 1998 American Institute of Physics. [S0003-6951(98)01432-6]

The topology and the physicochemical properties of polymer surfaces after ultraviolet (UV)-laser irradiation have been intensely studied for the past 15 years.<sup>1,2</sup> Irradiation with fluences below and around the ablation threshold,  $\phi < \phi_{th}$ , results in various surface modifications, such as amorphization, chemical degradation, instabilities and structure formation, etc. With fluences  $\phi > \phi_{th}$ , surface degradations and topological changes become more pronounced, and real ablation (material removal) is observed. However, the microscopic mechanisms for ablation, and in particular, the relative importance of thermal and nonthermal contributions, including defect and stress formation, are still under discussion. Experimentally, UV-laser ablation of organic polymers has been studied *mainly* by using excimer lasers which have pulse lengths of 10–30 ns.<sup>1,2</sup> Multiple-pulse ablation rates are typically measured as a function of laser fluence and wavelength, at laser spot sizes of  $2w \approx 100$   $\mu$ m.

The data derived from such experiments, however, do *not* permit a proper analysis of the fundamental interaction mechanisms because:

- (i) Photochemical processes should depend on the product of the intensity and the time of exposure,  $I\tau_p$ , while photo-physical and thermal processes depend heavily on  $\tau_p$ .
- (ii) Multiple-pulse irradiation changes the physical and chemical properties of the material, so that the material parameters which determine the ablation rate change during the ablation process, for example, due to the generation of absorbing defects (incubation centers).
- (iii) With ns pulses and large laser-spot sizes, the shielding of the incident laser beam by the ablation plume cannot be ignored.

In this letter we report on single-shot experiments using focused UV-Ar<sup>+</sup>-laser radiation ( $\lambda_c = 302$  nm,  $\Delta\lambda = 9$  nm,  $I = I_0 \exp[-(r/w_0)^2]$ ,  $w_0 \approx 2.6 \pm 0.2$   $\mu$ m). Here, the fluence  $\phi_0 = I_0\tau_p$  is changed either via the laser beam intensity,  $I_0$ , or via the pulse length,  $\tau_p$ . The pulse length was controlled by a digitally driven acousto-optic modulator. By this means, almost rectangular laser pulses with 140 ns  $\leq \tau_p \leq 50$  ms full width at half maximum were generated.<sup>3,4</sup> For a tight focus and relatively long  $\tau_p$ , the expansion of the vapor plume is essentially three-dimensional, and plasma shielding effects

can be ignored. The experimental data presented permit one to separate basic interaction mechanisms from influences of physical and chemical changes related to multiple-pulse irradiation. The changes in surface topology and the ablated depth have been studied by atomic force microscopy (AFM). In contrast to mass loss measurements using a quartz-crystal microbalance,<sup>5</sup> the present technique permits one to investigate the real surface profile near the ablation threshold.

Localized irradiation of polyimide (PI) with subthreshold fluences  $\phi_0 \leq \phi_{th}$ , results in the formation of a hump as shown in Fig. 1(a). Hump formation has been tentatively explained by amorphization of the material *and* an additional volume increase related to relatively large polymer fragments which are trapped within the surface.<sup>6</sup> This creates an internal pressure within the polymer, which may cause a swelling of the surface. Smaller fragments, such as CO, CN, C, C<sub>2</sub>, CH, C<sub>2</sub>H<sub>2</sub>, etc., are released from the sample.

Subsequently, we concentrate on the regime  $\phi_0 \approx \phi_{th}$  where real ablation starts. Here, we define the threshold flu-

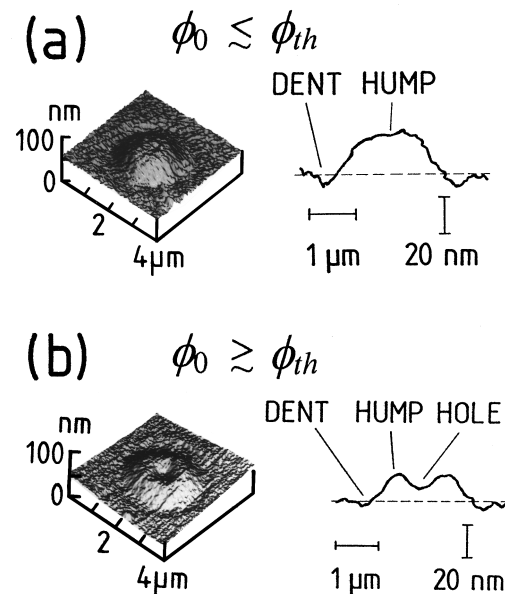


FIG. 1. UV laser-induced surface topology changes on PL. The fluence on the surface was of Gaussian shape with  $w_0 \approx 2.1$   $\mu$ m: Left: AFM pictures (three-dimensional view). Right: cross sections. (a)  $\phi_0/\phi_{th} \approx 0.96$ ,  $\tau_p = 5$   $\mu$ s; and (b)  $\phi_0/\phi_{th} \approx 1.01$ ,  $\tau_p = 2.1$   $\mu$ s.

<sup>a)</sup>Electronic mail: dieter.baeuerle@jk.uni-linz.ac.at

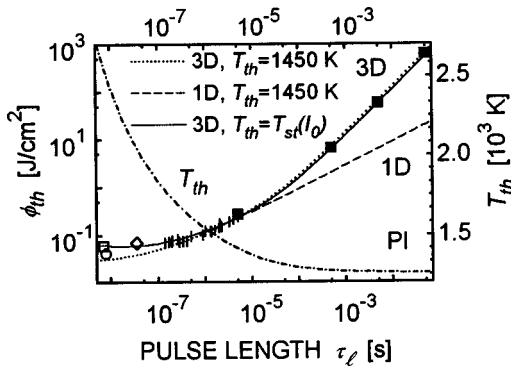


FIG. 2. Dependence of the threshold fluence for ablation on Ar<sup>+</sup>-laser pulse duration ( $\lambda \approx 302$  nm). ■ present work; | Refs. 3 and 4; □ Ref. 7; ◇ Ref. 8; and ○ Ref. 9. Dotted curve: 3D heat transport and constant temperature,  $T_{th} = 1450$  K. Dashed curve: 1D heat transport. For short pulses, this curve coincides with the dotted curve. Full curve: 3D heat transport with  $T_{th} = T_{st}(I_0)$ ; the dash-dotted curve shows the corresponding dependence of  $T_{th}$  on  $\tau_l$ .

ence for ablation by the average of the lowest fluence at which a dip appears in the center of the hump [Fig. 1(b)] and the highest fluence for which this dip is absent [Fig. 1(a)]. Figure 2 shows the threshold fluence  $\phi_{th}$  as a function of  $\tau_l$ . Full symbols were derived from the experiments described in this letter. Vertical bars refer to our earlier measurements<sup>3,4</sup> and open symbols to values found in the literature.<sup>7-9</sup> The experiments in Refs. 3 and 4 were done with  $w_0 = 2.1$   $\mu\text{m}$ , but with the short pulses used there heat conduction is one-dimensional, and  $w_0$  does not influence the  $\phi_{th}(\tau_l)$  dependence. Figure 2 demonstrates that  $\phi_{th}$  is almost constant with pulse lengths up to  $\tau_l \leq 200$  ns. Thus, experiments within this range are *not* conclusive with respect to the ablation mechanisms. For longer pulses, however, a strong increase in  $\phi_{th}$  with  $\tau_l$  is observed. With  $\tau_l > 100$   $\mu\text{s}$ ,  $\phi_{th}$  increases almost linearly with  $\tau_l$ . This dependence of  $\phi_{th}$  on  $\tau_l$  is a strong indication that ablation with 302 nm radiation *cannot* be based on a (purely) photochemical process.

If, on the other hand, we assume a purely *thermal* process, ablation should start, in a *first* approximation, at around the *same* threshold temperature  $T_{th}$ . For a Gaussian intensity profile, the laser-induced temperature rise is given by [Eq. (7.5.1) in Ref. 1]

$$\Delta T_{th} \equiv T_{th} - T(\infty) = \frac{w_0 A}{\kappa} \frac{\phi_{th}}{\tau_l} \int_0^{\tau_l^*} \frac{\alpha^*}{1 + 4t^*} \times \exp(\alpha^{*2} t^*) \operatorname{erfc}(\alpha^* t^{*1/2}) dt^*, \quad (1)$$

where  $t^* = tD/w_0^2$  and  $\alpha^* = \alpha w_0$ .  $T(\infty) = 300$  K is the background temperature,  $A$  the absorptivity,  $D$  the thermal diffusivity,  $\alpha$  the absorption coefficient, and  $\kappa$  the thermal conductivity. For PI, we employ  $D = 7.5 \times 10^{-4}$   $\text{cm}^2/\text{s}$ ,  $\kappa = 2.13 \times 10^{-3}$  W/cm K,  $A = 0.89$ ,  $w_0 = 2.5$   $\mu\text{m}$ , and  $\alpha = 1.5 \times 10^5$   $\text{cm}^{-1}$ .<sup>10</sup> With these parameters and for a certain pulse length  $\tau_l$  and the measured threshold fluence  $\phi_{th}(\tau_l)$ , we derive from Eq. (1) a center temperature of  $T_{th} = 1450 \pm 50$  K. With the assumption that ablation always starts at this center temperature, we can calculate from Eq. (1) the dependence  $\phi_{th} = \phi_{th}(\tau_l)$ . This is shown in Fig. 2 by the dotted curve. The agreement between the experimental data

and the calculated curve is quite satisfactory for pulse lengths  $\tau_l > 200$  ns. For very long pulse lengths  $\tau_l^* \gg 1$ , and surface absorption  $\alpha^* \gg 1$ , Eq. (1) yields

$$\phi_{th} \approx \frac{2}{\sqrt{\pi}} [T_{th} - T(\infty)] \frac{\kappa \tau_l}{A w_0}. \quad (2)$$

This describes the linear behavior of the dotted curve with long laser pulses.

The dependence expected in the limit of one-dimensional (1D) heat diffusion can as well be derived from Eq. (1). With large values of  $w_0$ , i.e.,  $\tau_l^* \ll 1$ , we obtain

$$\Delta T_{th} = \frac{A}{\alpha \kappa} \frac{\phi_{th}}{\tau_l} \left[ \frac{2}{\sqrt{\pi}} (D \alpha^2 \tau_l)^{1/2} + \exp(D \alpha^2 \tau_l) \operatorname{erfc}[(D \alpha^2 \tau_l)^{1/2}] - 1 \right]. \quad (3)$$

This dependence is depicted in Fig. 2 by the dashed curve. For short pulse lengths this curve coincides with the dotted curve. In the limit of strong absorption, i.e., with  $\alpha^* \gg 1$ , this yields

$$\phi_{th} \approx [T_{th} - T(\infty)] \frac{(\pi \kappa c_p \rho)^{1/2}}{2A} \tau_l^{1/2}, \quad (4)$$

where  $\rho$  is the mass density and  $c_p$  the specific heat of PI. Figure 2 shows that with the parameters employed, three-dimensional (3D) and 1D curves start to diverge with pulse lengths  $\tau_l > 10$   $\mu\text{s}$ .

It is evident that the preceding description is too simple: First, the calculated dependence  $\phi(\tau_l)$  may change due to the temperature dependence of the material parameters.<sup>10</sup> In the region of very short pulses, where heat conduction is unimportant, we can employ the calorimetric solution

$$c_p \rho \frac{dT}{dt} = A \alpha I, \quad (5)$$

which yields

$$\phi_{th} = \int_{T(\infty)}^{T_{th}} \frac{c_p(T) \rho(T)}{A(T) \alpha(T)} dT. \quad (6)$$

Thus, even when we assume  $T_{th} = \text{constant}$ , an increase in  $c_p$  and/or a decrease in  $\alpha$  may explain the discrepancy between the experimental data and the dotted curve in the ns range. Note that  $c_p$ ,  $\rho$ , and  $\alpha$  *do not* influence the dependence  $\phi_{th}(\tau_l)$  for *long* pulses, which is given by Eq. (2). This proves to be true even for temperature-dependent parameters.  $A(T)$  influences  $\phi_{th}$  in a similar way for all  $\tau_l$ .

Second, the temperature  $T_{th}$  is in reality not constant, but increases with decreasing laser pulse length. With the assumption that ablation is a thermally activated *surface* process, the velocity of the ablation front can be described by the Arrhenius-type law

$$v = v(T) = v_0 \exp(-T_a/T), \quad (7)$$

where  $T$  is the surface temperature and  $T_a = \Delta E_V/k_B$  the activation temperature. Because the time for ablation decreases with decreasing pulse duration,<sup>1</sup> ablation of a certain layer thickness requires higher ablation velocities, and thus higher temperatures. Let us adopt a simplified picture: In the

beginning of the pulse, the material is only heated and  $v = 0$ . When ablation starts, the velocity  $v$  reaches its stationary value immediately; this is a good approximation for a high activation temperature  $T_a$ , and for pulse durations long compared to the transition to stationary ablation. For PI, this is fulfilled for  $\tau_p > 100$  ns.<sup>1,11–13</sup> Within this picture, the threshold temperature equals the temperature for stationary ablation, i.e.,  $T_{th} = T_{st} \equiv T_{st}(I_0)$ .  $T_{st}$  can be calculated as follows: Let us consider a small displacement  $v dt$  by which the ablation front moves with a constant velocity  $v$ . In a reference frame fixed in the moving surface, the laser-induced temperature distribution within the material remains constant, and the energy balance for the time interval  $dt$  is

$$AI_0 dt = \rho v dt [H_V(T_{st}) + H(T_{st})]. \quad (8)$$

The first term in the brackets represents the latent heat of vaporization, the second describes the enthalpy change related to the temperature change  $T_{st} - T(\infty)$  of the layer  $v dt$ . With materials that melt, one has to add the latent heat of fusion. At moderate temperatures, the temperature dependence of  $H_V$  can be approximated by

$$H_V(T_{st}) \approx H_V + H_g(T_{st}) - H(T_{st}), \quad (9)$$

where  $H_V \equiv H_V[T(\infty)]$ .<sup>14</sup>  $H_g$  is the enthalpy of the gas phase with respect to  $T(\infty)$ . With Eq. (9) we obtain from Eq. (8)

$$AI_0 \approx \rho v \tilde{H}, \quad (10)$$

where

$$\tilde{H}(T_{st}) \equiv H_V + H_g(T_{st}) = H_V + \int_{T(\infty)}^{T_{st}} c_g(T) dT.$$

This equation represents the energy conservation law in 1D stationary ablation. Equation (10) can even be employed when  $\tilde{H}$  includes the kinetic energy of ablated species and chemical reaction enthalpies. Equations (7) and (10) allow one to calculate  $T_{st}$  and  $v$  for given values of  $I_0$ . With  $T_{th} \equiv T_{st}$ , one can calculate from Eq. (1) the corresponding values of  $\tau_p$ , and thus,  $\phi_{th} \equiv I_0 \tau_p$ . The dash-dotted curve in Fig. 2 shows the dependence  $T_{th}(\tau_p)$ , and the full curve the dependence  $\phi(\tau_p)$ . Here, the parameters  $T_a = 1.65 \times 10^4$  K,  $\tilde{H} = 3.3$  kJ/g, and  $v_0 = 10^6$  cm/s have been employed.

The approximation  $T_{th} = T_{st}(I_0)$  leads to an increase in  $T_{th}$ , which is roughly logarithmic with intensity and is most pronounced with short pulses. As a consequence, in this region the experimental data are described better by the full curve. With ns pulses, however, the stationary regime will not be reached, and the results become more sensitive to temperature dependences in the material parameters and to the exact kinetics of the ablation process.

With long pulses, the full curve almost coincides with the dotted curve. In this region, 3D heat transport dominates and the temperature distribution is almost stationary. Then, one can introduce the linearized temperature<sup>1</sup>  $\theta$ , and substitute  $\kappa[T_{th} - T(\infty)]$  in Eq. (2) by

$$\kappa[T(\infty)] \theta(T_{th}) \equiv \int_{T(\infty)}^{T_{th}} \kappa(T) dT. \quad (11)$$

This preserves the linear dependence  $\phi_{th}(\tau_p)$ . If we divide Eq. (2) by  $\tau_p$  and eliminate  $I_0$  together with Eqs. (10) and (7) for  $T \equiv T_{th}$ , we end up with an equation for  $T_{th}$  only.

Thus, with long pulses  $T_{th}$  is indeed constant. This holds even with finite absorption  $\alpha w_0$  and  $\alpha = \alpha(T)$ ,  $A = A(T)$ . Finally, the stationary ablation condition (10) should be corrected to take into account 3D effects. This has been investigated using the approximation of parabolic ablation front.<sup>15</sup> However, with the parameters employed above, no significant deviations from the full curve were found.

The excellent agreement between the experimental data and the model calculations is a strong indication that changes in the material properties, e.g., due to carbonization (Ref. 16) can be ignored in single-pulse experiments with fluences near  $\phi_{th}$ . In fact, ablation of carbonized material,<sup>17,18</sup> would require higher  $T_{th}$ , especially for long pulses, in contrast to our analysis which shows a decrease in  $T_{th}$ .

In summary, we can say that the experimental data presented in this letter demonstrate a strong dependence of the threshold fluence for ablation,  $\phi_{th}$ , on laser pulse duration,  $\tau_p$ . Within the range of pulse lengths investigated,  $10$  ns  $< \tau_p < 50$  ms, the experimental data can be well described by a purely thermal model. The experimental results reveal that for PI a clear distinction between thermal and photochemical mechanisms becomes possible only if one investigates pulse durations  $\tau_p > 100$  ns. In this regime, the heat penetration depth exceeds the optical penetration depth.

This work was supported by the ‘‘Fonds zur Förderung der Wissenschaftlichen Forschung in Österreich.’’

<sup>1</sup>D. Bäuerle, *Laser Processing and Chemistry* (Springer, Heidelberg, 1996).

<sup>2</sup>R. Srinivasan, in *Laser Ablation*, edited by J. C. Miller, Springer Ser. Mater. Sci., Vol. 28 (Springer, Berlin, 1994), p. 107.

<sup>3</sup>M. Himmelbauer, Ph.D. dissertation, Linz, 1996.

<sup>4</sup>M. Himmelbauer, E. Arenholz, and D. Bäuerle, Appl. Phys. A: Mater. Sci. Process. 63A, 87 (1996).

<sup>5</sup>S. Küper, J. Brannon, and K. Brannon, Appl. Phys. A: Solids Surf. A56, 43 (1993).

<sup>6</sup>M. Himmelbauer, E. Arenholz, D. Bäuerle, and K. Schilcher, Appl. Phys. A: Mater. Sci. Process. 63A, 337 (1996).

<sup>7</sup>J. E. Andrew, P. E. Dyer, D. Forster, and P. H. Key, Appl. Phys. Lett. 43, 717 (1983).

<sup>8</sup>J. H. Brannon, J. R. Lankard, A. I. Baise, F. Burns, and J. Kaufman, J. Appl. Phys. 58, 2036 (1985).

<sup>9</sup>P. E. Dyer and J. Sidhu, J. Appl. Phys. 57, 1420 (1985).

<sup>10</sup>Du Pont, Inc., *Kapton Polyimide Film-Summary of Properties* (1988).

<sup>11</sup>D. Bäuerle, B. Luk'yanchuk, P. Schwab, X. Z. Wang, and E. Arenholz, in *Laser Ablation of Electronic Materials*, edited by E. Fogarassy and S. Lazare (Elsevier, Amsterdam, 1992), p. 39.

<sup>12</sup>B. Luk'yanchuk, N. Bituyurin, M. Himmelbauer, and N. Arnold, Nucl. Instrum. Methods Phys. Res. B 122, 347 (1997).

<sup>13</sup>N. Arnold, B. Luk'yanchuk, and N. Bituyurin, Appl. Surf. Sci. 127, 184 (1998).

<sup>14</sup>L. D. Landau and E. M. Lifshitz, *Course of Theoretical Physics*, Vol. 5, *Statistical Physics*, Part 1 (Pergamon, Oxford, 1980).

<sup>15</sup>E. I. Sobol, *Phase Transformations and Ablation in Laser-Treated Solids* (Wiley, New York, 1995).

<sup>16</sup>R. Srinivasan, R. R. Hall, W. D. Loehle, W. D. Wilson, and D. C. Allbee, J. Appl. Phys. 78, 4881 (1995).

<sup>17</sup>Z. Ball, T. Feurer, D. L. Callahan, and R. Sauerbrey, Appl. Phys. A: Mater. Sci. Process. 62A, 203 (1996).

<sup>18</sup>S. Lazare, W. Guan, and D. Drilhole, Appl. Surf. Sci. 96-98, 605 (1996).